Hindawi
Journal of Nanotechnology
Volume 2022, Article ID 7971119, 6 pages
https://doi.org/10.1155/2022/7971119

Research Article

Optical Investigation of p-GaAs/i-$GaN_{0.38y}As_{1-1.38y}Sb_y$/n-GaAs Quantum Wells Emitters

I. Guizani[1], **C. Bilel**[2], **Malak Alrowaili**[2] **and A. Rebey**[3]

[1]*Physics Department, Faculty of Sciences and Arts in Qurayyat, Jouf University, Sakaka, Jouf, Saudi Arabia*
[2]*Physics Department, College of Science, Jouf University, P.O. Box 2014, Sakaka, Saudi Arabia*
[3]*Physics Department, College of Science- Buraydah, Qassim University, Buraidah, Saudi Arabia*

Correspondence should be addressed to I. Guizani; iguizanii@gmail.com and C. Bilel; chakroun@ju.edu.sa

Received 31 October 2021; Revised 22 March 2022; Accepted 24 March 2022; Published 13 April 2022

Academic Editor: Sivakumar Manickam

We have studied the 1.55 μm optical properties of p-GaAs/i-$GaN_{0.38y}As_{1-1.38y}Sb_y$/n-GaAs quantum wells using a self-consistent calculation combined with the anticrossing model. We have found that the increase of injected carriers' density induces the increase of optical gain and radiative current density. The rise of doping density causes a blue shift of the fundamental transition energy accompanied with significant increase of optical gain. The quantum-confined Stark effect on radiative current density is also studied. The variation of radiative current as function of well width and Sb composition is also examined. In order to operate the emission wavelength at the optical fiber telecommunication domain, we have adjusted the well parameters of p-GaAs/i-$GaN_{0.38y}As_{1-1.38y}Sb_y$/n-GaAs.

1. Introduction

Antimony-based III-V semiconductors have a great interest in the field of optoelectronics for the design of long wavelength infrared detection devices [1–3]. In fact, these compounds reveal motivated electrical and optical properties, especially a significant reduction of the gap covering the telecom and the long infrared domains [4, 5]. Technological progress in growth techniques, such as molecular beam epitaxy (MBE) and metal organic chemical vapor deposition, offers the opportunity to control the incorporation of small Sb or N amounts into GaAs host matrix. In fact, the incorporated N atom induces a strong band gap reduction around 180 meV/%N [6–10]. As proof of this behavior, Chakir et al. [7] have studied the band structure reconstruction of $GaAs_{1-x}N_x$ using the 10×10 band anticrossing (BAC) model. Similarly, the incorporation of Sb leads to a band gap reduction of about 16 meV/%Sb [11, 12]. Alberi et al. [11] have used the 12×12 BAC model to calculate the valence bands in $GaAs_{1-x}Sb_x$ material. Consequently, the simultaneous incorporation of N and Sb into GaAs matrix accelerates the ratio of the band gap reduction. Experimental reported works [12–15] indicate that the band gap of $GaAs_{0.89}N_{0.03}Sb_{0.09}$ material reaches a low value of 0.835 eV. Also, many research groups have succeeded in developing thin film structures based on GaAs1-x-yNxSby for telecommunication in the optical windows 1.3 and 1.55 μm characterized by high transmission. Indeed, Harmand et al. [16, 17] reported the elaboration of high crystalline $GaN_xAs_{1-x-y}Sb_y$/GaAs structures with wavelength emission 1.3–1.55 μm. They stated the improvement of photoluminescence property after thermal annealing. Lin et al. [18] and Lourenço et al. [19] elaborated 1.3 μm (i.e., 0.95 eV) $GaN_xAs_{1-x-y}Sb_y$/GaAs structures. The energy band diagram of GaAsSbN has been computed by using the double BAC model consisting of a conduction BAC model and a valence BAC model. More advanced, Ohtani et al. [20] elaborated *n*-doped InAs/AlSb quantum structures using MBE. The doping effect on the optoelectronic properties of type II $GaAs_{.76}Sb_{.24}/In_{.26}Ga_{.74}N_{.06}As_{.94}$/GaAs QW was studied by Kim and Park [21]. Tan et al. [22] examined the optical absorption of the p-i-n GaNAsSb/GaAs structure emitting at 1.3 μm. They found that the absorption coefficient is about 1.3 10^4 cm^{-1}. Luo et al. [23] reported that the absorption coefficient of GaNAsSb/GaAs double-QWs emitting at $1.55\,\mu$m is equal to 2 $10^4\,\text{cm}^{-1}$.

The purpose of this work is to investigate the optical gain and radiative current density of $1.55\,\mu$m p-GaAs/i-$GaN_{0.38y}As_{1\text{-}1.38y}Sb_y$/n-GaAs quantum wells emitters. We examined the dependence of optical gain on the injected carrier density and doping effect. In addition, the applied electric field, well width, and Sb composition effects on the radiative current density are also discussed.

2. Theory

In this part, we detail a theoretical model used to calculate the electronic and optical properties of p-GaAs/i-$GaN_{0.38y}As_{1\text{-}1.38y}Sb_y$/n-GaAs quantum wells. For this particular structure, it should be noted that the x composition of nitrogen is chosen as $x = 0.38y$ that ensures zero mismatch between GaNAsSb alloy and GaAs substrate. In fact, we have used the (16×16) BAC model combined with self-consistent calculation. The Schrödinger equation is solved taking into account the band discontinuity between the GaAs barrier and GaNAsSb well ΔU. The Hartree potential $U_H(z)$ and the exchange-correlation potential $U_{xc}(z)$ are obtained by solving Poisson's equation. The term eFz is linked to the Stark effect [24, 25]:

$$\left(-\frac{\hbar^2}{2m^*_{e,h}}\nabla^2 + \Delta U(z) + U_H(z) + U_{xc}(z) + eFz\right)\varphi_k(z) = E_k\varphi_k(z),$$
$$\frac{d^2U_H(z)}{dz^2} = \frac{e^2}{\varepsilon_0\varepsilon_r}\left(p(z) - N_a(z) + N_d(z) - n(z)\right), \tag{1}$$

where $m^*_{e,h}$ is the effective masses of electrons or holes, E_k and φ_k are, respectively, the k^{th} energy level and the envelope wavefunction, $\varphi_k(z)$ satisfies the boundary condition at the interface $z_0 = 0$ and $z_0 = L_w$, $N_d(z)$ and $N_a(z)$ are, respectively, the ionized donor and acceptor doping concentrations, and $n(z)$ and $p(z)$ are the carrier densities of electrons and holes, respectively.

The optical performances for p-GaAs/i-$GaN_{0.38y}As_{1\text{-}1.38y}Sb_y$/n-GaAs QW laser structures are estimated in terms of optical gain and radiative current density. The optical gain calculated at photon energy E is obtained with the contribution of the fundamental transitions T_{ei-hi} for $k_p = 0$. It was described by the following expression [26, 27]:

$$G(E, E_p) = \frac{1}{L_w}\frac{e^2\hbar}{m_0^2 n\varepsilon_0 Ec}\sum_{i,j} I^{e_i}_{h_i}\int_0^\infty \rho^j_{i2\,D}\left|M^j_i(E_p)\right|^2\left(f^n_c(E_p) - f^m_v(E_p)\right)L^j_i(E, E_p)\,dE_p, \tag{2}$$

where C and ε_0 are, respectively, the velocity of light and permittivity of free space, $\boldsymbol{n}$ and L_w are the refractive index and well width, respectively, $I^{e_i}_{h_i}$ is the wave function envelope, ρ^j_{i2D} is the two-dimensional density state, $|M^j_i(E_p)|^2$ is the optical transition matrix element between heavy hole subband h_i and electron subband e_i for TE polarization, $L^j_i(E, E_p)$ is the Lorentzian line shape function, and $f^n_c(E_p)$ and $f^m_v(E_p)$ are, respectively, Fermi functions for the n^{th} subband in the conduction band and m^{th} subband in the valence band [28].

For an ideal laser without any nonradiative recombination processes, the radiative current density is given by the following formula [29]:

$$J_{\text{rad}} = eL_wBN_i^2, \tag{3}$$

where **B** and $\mathbf{N_i}$ are, respectively, the spontaneous radiative recombination coefficient and the injected carrier density [30].

$$B = \frac{e^2L_wnE_g\left|M_{avr}\right|^2}{m_0^2\varepsilon_0c^3k_bTm^*_h(1+r)}, \tag{4}$$

where $\boldsymbol{e}$ is the electron charge, E_g is the band gap energy, m_0 is the free electron mass, $|M_{avr}|^2$ is the average of the squared of the momentum matrix element, k_b is the Boltzmann constant, and $r = (m^*_e/m^*_h)$ is the ratio of the electron and hole effective masses [31].

3. Results and Discussion

The electronic band structure of p-GaAs/i-$GaN_{0.070}As_{0.743}Sb_{0.186}$/n-GaAs QW without and under an applied electric field $F = 40$kV/cm is shown in Figure 1. The donor and acceptor doping concentrations are equal to $2\times10^{18}\,\text{cm}^{-3}$ and $3\times10^{18}\,\text{cm}^{-3}$, respectively. All calculations were performed with temperature 300 K as the input parameter. The Sb composition and well thickness are equal to $y_{Sb} = 18.6\%$ and $L_w = 4$ nm, respectively.

Figure 2 shows the variation of maximum gain $G_{\max}$ and radiative current density J_{rad} as function of the injected carrier density $\mathbf{N_i}$ for p-GaAs/i-$GaN_{0.38y}As_{1\text{-}1.38y}Sb_y$/n-GaAs quantum well structures. The optimized well parameters give rise to $\lambda_{e_1-h_1} = 1.55\,\mu$m. By increasing the injected carrier

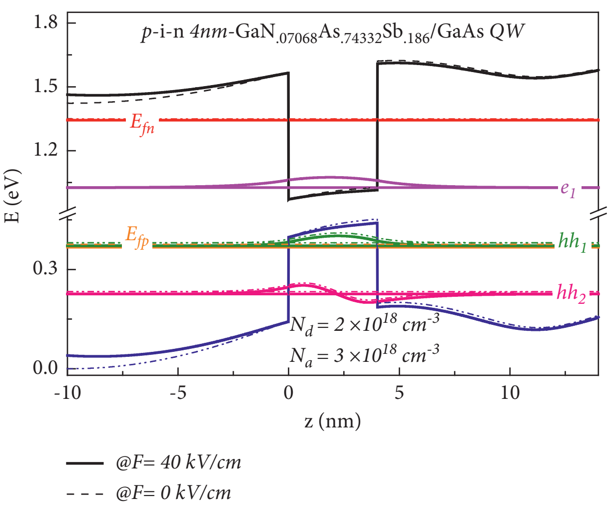

FIGURE 1: Band diagram of p-GaAs/i-$GaN_{0.070}As_{0.743}Sb_{0.186}$/n-GaAs QW without and under an applied electric field $F = 40$ kV/cm.

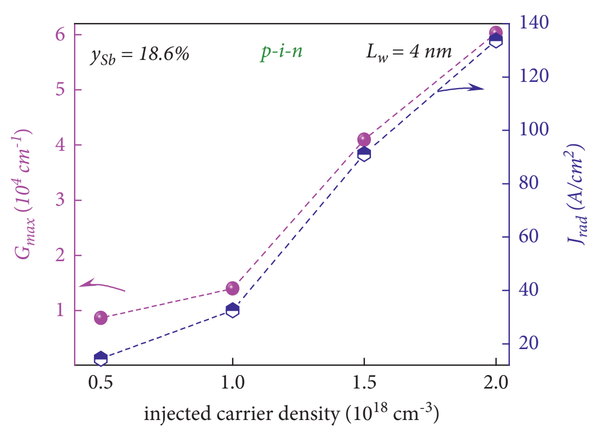

FIGURE 2: Optical gain and radiative current density as function of injected carriers density N_{inj} ranging from 5×10^{17} to 2×10^{18} cm^{-3} for p-GaAs/i-$GaN_{0.38y}As_{1-1.38y}Sb_y$/n-GaAs QW structure. The Sb composition and well width are y_{Sb} = 18.6% and L_w = 4 nm, respectively.

density from 5×10^{17} to 2×10^{18} cm^{-3}, the optical gain increases from 8.65×10^3 to 6×10^4 cm^{-3}. Likewise, the radiative current density magnitude rises from 14.41 to 133.7 A/cm^2. The same behavior was observed by Liu et al. [32]. They indicated an enhancement in optical gain varying the carrier concentrations from 8×10^{18} to 2.4×10^{19} cm^{-3} for GaAsSb/GaAs quantum well lasers. Furthermore, Park et al. [33] studied the optical gain as functions of carrier density and the radiative current density for the GaAsSbN/GaAs QW structures emitting at 1.3 μm wavelength. They showed that optical gain in GaAsSbN/GaAs QW structures is about 2.8×10^3 cm^{-3}, which is higher than GaAsSb/GaAs QW. They also illustrated that the radiative current density of GaAsSbN/GaAs is nearly the same as that of the InGaAsN/GaAs QW structure. In another study, Park et al. [34] reported the dependence of the optical gain on the carrier density for GaAsSbN/GaAs QW structures with several compressive strains. Chen et al. [35] studied the dependence of gain maximum of W structure with 3 nm compressively strained $GaAs_{0.35}Sb_{0.65}$ layers for three different carriers' concentrations. For 3 nm InGaAs/3 nm GaAsSbBi QW [36], TE material gain increases when the carrier concentration varies from 2×10^{18} to 6×10^{18} cm^{-3}.

The calculated optical gain for doped GaNAsSb well for p-GaAs/i-$GaN_{0.38y}As_{1-1.38y}Sb_y$/n-GaAs quantum well laser is shown in Figure 3. It was significantly enhanced from 4×10^3 to 9.6×10^3 cm^{-3} with increasing doping density from 5×10^{16} to 1.5×10^{17} cm^{-3}. Similarly, Kim et al. [21] reported the increase of optical gain as function of doping densities of the $GaSb_{0.24}As_{0.76}/In_{0.26}Ga_{0.74}N_{0.06}As_{0.94}$/GaAs QW structure. They claim that this behavior can be explained by the fact that the optical matrix element increases with increasing doping density. Jiang et al. [37] examined the gain spectra for TE-polarized light, the n-doped Ge/GeSi quantum well under various n-type doping concentrations. They indicated that at low strain level, the optical gain could be enhanced when n-type doping concentration increases from 5×10^{18} to 5×10^{19} cm^{-3}. On the other hand, Huang et al. [38] studied the variation of maximum gain of $Ge_{0.9375-m}Sn_{0.0625}P_m$, $Ge_{0.9375-m}Sn_{0.0625}As_m$, $Ge_{0.9375-m}Sn_{0.0625}Sb_m$, and $Ge_{0.9375-m}Sn_{0.0625}Bi_m$ as a function of doping concentration for an injected carrier density of 1×10^{19} cm^{-3}. They illustrated that the gain increase as function of the doping concentration, and the effects of the doping elements on the optical gain of GeSn can be ranked as Bi > Sb > As > P.

We investigated the effect of the applied electric field on the radiative current density for p-GaAs/i-$GaN_{0.38y}As_{1-1.38y}Sb_y$/n-GaAs QW structure operating at 1.55 μm telecommunication wavelength, as shown in Figure 4. The antimony composition and well thickness are y_{Sb} = 18.6% and L_w = 4.1 nm, respectively. The calculated radiative current increases from 67.07 to 102.64 A/cm^2 when F changes from 0 up to 40 kV/cm. This behavior was stated in our previous work [39] for p-GaAs/i-GaNAsBi/n-GaAs QWs. We mentioned that the radiative current density varies from 101.3 to 515.3 A/cm^2, with increasing the electric field from 0 up to 40 kV/cm. The rise of the current density is also indicated by Mensfoort et al. [40] for blue polymer-based light-emitting diodes. They interpret this increase by the improvement of the net space charge density caused by the reduced recombination rate for small voltages.

The radiative current density J_{rad} as well as the fundamental transition energy as function of well width L_w is shown in Figure 5(a). J_{rad} increases from 37.81 to 151.04 A/cm^2. The increase of L_w from 4 to 4.5 nm induces a significant red-shift of fundamental transition energy from 802 to 774 meV. In another study, Bilel et al. [41] stated that the shift of the fundamental transition energy $T_{e1\text{-}h1}$ to lower energies can be explained by the modification of the electron and hole subbands under the effect of the applied electric field. To correct this shift, we adjusted the Sb composition y_{Sb} for each used value of well width L_w. The optimized values of y_{Sb} are, respectively, equal to 17.8 and 18.8% for 4 and 4.5 nm, as shown in Figure 5(b). The radiative current density varies 47 from to 144.7 A/cm^2 at 1.55 μm telecommunication wavelength.

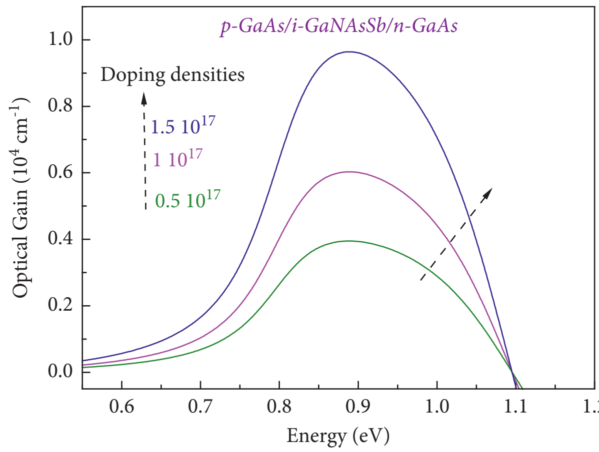

FIGURE 3: Optical gain as function of energy for different doping densities for p-GaAs/i-$GaN_{0.38y}As_{1-1.38y}Sb_y$/n-GaAs QW laser structure with N_D equal to 5×10^{16}, 1×10^{17}, and 1.5×10^{17} cm^{-3}. The Sb composition and well width are y_{Sb} = 18.6% and L_w = 4 nm, respectively.

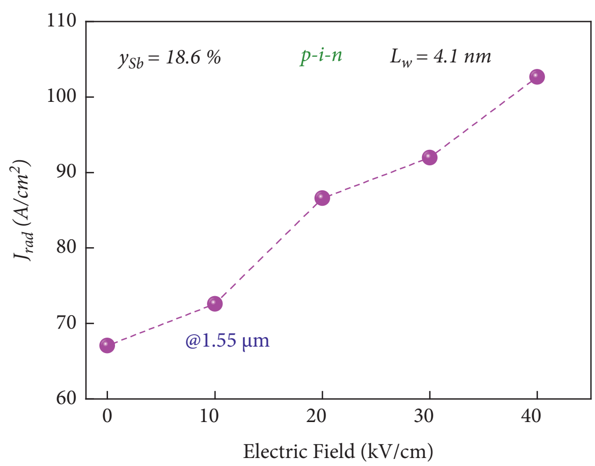

FIGURE 4: The radiative current density as function of applied electric field F varying from 0 up to 40 kV/cm for p-GaAs/i-$GaN_{0.38y}As_{1-1.38y}Sb_y$/n-GaAs QW structure operating at 1.55 μm telecommunication wavelength. The Sb composition and the well width are y_{Sb} = 18.6% and L_w = 4.1 nm, respectively.

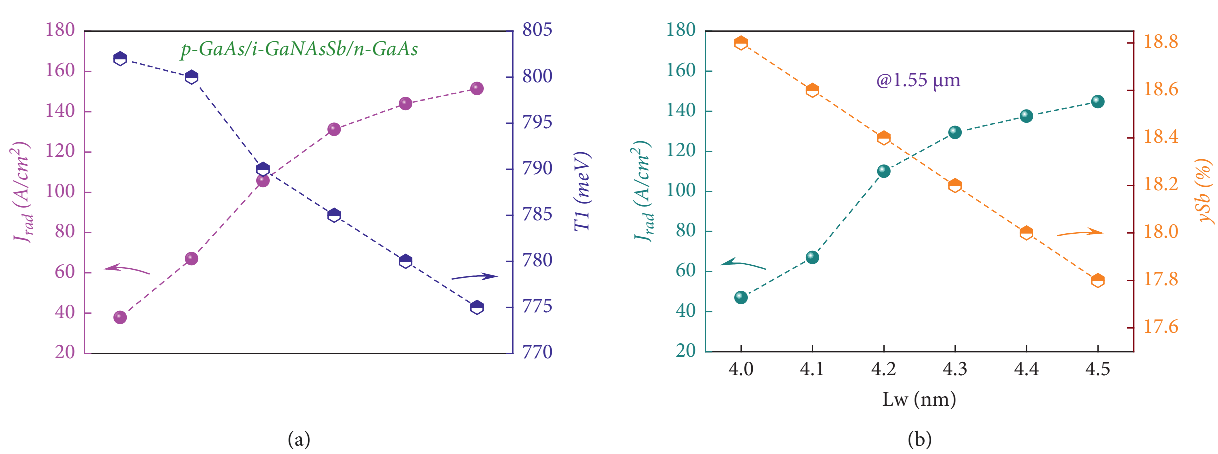

FIGURE 5: (a) Variation of radiative current density and fundamental energy transition as function of well width. (b) The adjusted value of Sb composition and radiative current density at 1.55 μm.

Such optimization of the well parameters (well thickness and Sb composition) seems to be interesting investigation to enhance the optoelectronic performance of 1.55 μm p-GaAs/i-$GaN_{0.38y}As_{1-1.38y}Sb_y$/n-GaAs quantum wells emitters.

4. Conclusion

The optoelectronic properties of 1.55 μm p-GaAs/i-$GaN_{0.38y}As_{1-1.38y}Sb_y$/n-GaAs quantum wells were theoretically investigated using a self-consistent calculation combined with an anticrossing model. The maximum of gain is enhanced with increasing the injected carrier density. The optical gain reaches the value $9.6 \times 10^3\,cm^{-1}$ for doping density equal to $1.5 \times 10^{17}\,cm^{-3}$. Moreover, the applied electric field significantly affects the radiative current density of the studied structure. The radiative current density is about 151.04 A/cm^2 for 4.5 nm well width. The fundamental transition energy $T_{e1\text{-}h1}$ shifts from 28 meV to lower energies when the well width varies from 4 to 4.5 nm. We can conclude that the obtained results are advantageous to the design of p-i-n based GaNAsSb quantum well laser structures operating at 1.55 μm telecommunication wavelength.

Data Availability

The datasets used to support the findings of this study are available from the corresponding author upon request.

Conflicts of Interest

The authors declare that there are no conflicts of interest.

Acknowledgments

The authors would like to thank the Deanship of Graduate Studies at Jouf University for funding and supporting this research through the initiative of DGS, Graduate Students Research Support (GSR) at Jouf University, Saudi Arabia.

References

[1] Y. Wei, A. Gin, and M. Razeghi, "Advanced InAs/GaSb superlattice photovoltaic detectors for very long wavelength infrared applications," *Applied Physics Letter*, vol. 80, p. 3262, 2002.

[2] C. Jin, J. Chen, Q. Xu, C. Yu, and L. He, "Electrical and optical performances of InGaAs/GaAsSb superlattice short-wavelength infrared detectors," *Optical Engineering*, vol. 56, no. 5, Article ID 057102, 2017.

[3] P. Deshmukh, J. Li, S. Nalamati, M. Sharma, and S. Iyer, "Molecular beam epitaxial growth of GaAsSb/GaAsSbN/GaAlAs core-multishell nanowires for near-infrared applications," *Nanotechnology*, vol. 30, p. 275203, 2019.

[4] L. Ma, X. Zhang, H. Li et al., "Bandgap-engineered GaAsSb alloy nanowires for near-infrared photodetection at 1.31 μm," *Semiconductor Science Technology*, vol. 30, Article ID 105033, 2015.

[5] E. Ahmad, M. Karim, S. Bin Hafiz, C. L. Reynolds, Y. Liu, and S. Iyer, "A two-step growth pathway for high Sb incorporation in GaAsSb nanowires in the telecommunication r-wavelength range," *Scientific Reports*, vol. 7, Article ID 10111, 2017.

[6] J. Wu, W. Shan, and W. Walukiewicz, "Band anticrossing in highly mismached III-V semiconductors alloys," *Semiconductor Science Technology*, vol. 17, p. 860, 2002.

[7] K. Chakir, C. Bilel, M. M. Habchi, A. Rebey, and B. El Jani, "Theoretical study of the carrier effective mass in diluted III-N-V semiconductor alloys using 10-band k.p model," *Thin Solid Films*, vol. 630, no. 25, 2017.

[8] I. Vurgaftman and J. R. Meyer, "Band parameters for nitrogen-containing semiconductors," *Journal of Applied Physics*, vol. 94, no. 6, pp. 3675–3696, 2003.

[9] K. Uesugi, N. Morooka, and I. Suemune, "Reexamination of N composition dependence of coherently grown GaNAs band gap energy with high-resolution x-ray diffraction mapping measurements," *Applied Physics Letter*, vol. 74, p. 1254, 1999.

[10] W. Shan, W. Walukiewicz, K. M. Yu et al., "Band anticrossing in III–N–V alloys," *Physical Status Solidi B*, vol. 223, p. 75, 2001.

[11] K. Alberi, J. Wu, W. Walukiewicz et al., "Valence-band anticrossing in mismatched III-V semiconductor alloys," *Physical Review B*, vol. 75, Article ID 045203, 2007.

[12] R. Teissier, D. Sicault, J. C. Harmand, G. Ungaro, G. Le Roux, and L. Largeau, "Temperature-dependent valence band offset and band-gap energies of pseudomorphic GaAsSb on GaAs," *Journal of Applied Physics*, vol. 89, p. 5473, 2001.

[13] K. I. Lin, K. L. Lin, B. W. Wang, H. H. Lin, and J. S. Hwang, "Double-band anticrossing in GaAsSbN induced by nitrogen and antimony incorporation," *Applied Physical Express*, vol. 6, Article ID 121202, 2013.

[14] N. Ben Sedrine, C. Bouhafs, J. C. Harmand, R. Chtourou, and V. Darakchieva, "Effect of nitrogen on the GaAs0.9−xNxSb0.1 dielectric function from the near-infrared to the ultraviolet," *Applied Physical Letter*, vol. 97, Article ID 201903, 2010.

[15] C. Z. Zhao, H. F. Guo, T. Wei, S. S. Wang, and K. Q. Lu, "Composition dependence of the band gap energy for the dilute nitride and as-rich GaNxSbyAs1−x−y ($0 \le x \le 0.05$, $0 \le y \le 0.3$)," *Physica B: Physics Conductor Matter*, vol. 485, no. 35, 2016.

[16] J. C. Harmand, G. Ungaro, J. Ramos et al., "Investigations on GaAsSbN/GaAs quantum wells for 1.3–1.55 μm emission," *Journal of Crystal Growth*, vol. 227, p. 553, 2001.

[17] J. C. Harmand, A. Caliman, E. V. K. Rao et al., "GaNAsSb: how does it compare with other dilute III–V-nitride alloys," *Semiconductor Science Technology*, vol. 17, Article ID 778, 2002.

[18] Y. T. Lin, T. C. Ma, T. Y. Chen, and H. H. Lin, "Energy gap reduction in dilute nitride GaAsSbN," *Applied Physics Letter*, vol. 93, Article ID 171914, 2008.

[19] S. A. Lourenço, I. F. L. Dias, L. C. Poças, J. L. Duarte, J. B. B. de Oliveira, and J. C. Harmand, "Effect of temperature on the optical properties of GaAsSbN/GaAs single quantum wells grown by molecular-beam epitaxy," *Journal of Applied Physics*, vol. 93, Article ID 4475, 2003.

[20] K. Ohtani, N. Matsumoto, H. Sakuma, and H. Ohno, "Intersubband absorption in n-doped InAs/AlSb multiple-quantum-well structures," *Applied Physics Letter*, vol. 82, no. 37, 2003.

[21] J. J. Kim and S. H. Park, "Effects of modulation doping on the optical properties of a type-II 1.55-μm GaAsSb/InGaNAs/GaAs trilayer quantum-well structure," *Journal of the Korean Physical Society*, vol. 57, no. 826, 2010.

[22] K. H. Tan, S. F. Yoon, W. K. Loke et al., "High responsivity GaNAsSb p-i-n photodetectors at 1.3 μm grown by radio-frequency nitrogen plasma-assisted molecular beam epitaxy," *Optics Express*, vol. 16, pp. 7720–7725, 2008.

[23] H. Luo, J. A. Gupta, and H. C. Liu, "1.55 μm GaNAsSb photodetector on GaAs," *Applied Physics Letter*, vol. 86, Article ID 211121, 2005.

[24] I. Guizani, C. Bilel, M. M. Habchi, and A. Rebey, "Optical gain spectra of 1.55 mm GaAs/GaN.58yAs1-1.58yBiy/GaAs single quantum well," *Superlattice and Microstructure*, vol. 102, p. 141, 2017.

[25] I. Guizani, K. Chakir, M. M. Habchi, and A. Rebey, "Investigation of optical gain in 1.55 μm p-i-n GaNAsBi-based DQWs," *Physical Status Solidi C*, vol. 14, Article ID 1700163, 2017.

[26] A. M. Khan, "Tuning of gain spectra in GaAsSb/InGaAsHeterostructure," *AIP Conference Proceedings*, vol. 2220, Article ID 020008, 2020.

[27] S. H. Park, H. M. Kim, and J. J. Kim, "Threshold current density of 1.3-μm GaAsSb/GaInAs/GaAs Type-II trilayer quantum well lasers on GaAs substrates," *Journal of the Korean Physical Society*, vol. 50, Article ID 1018, 2007.

[28] C. Lok, L. YanVoon, and M. Willatzen, *The k.P Method*, Springer, New York, NY, USA, 2009.

[29] E. S. Kzal Mohammed Qader, "Threshold courant density of Al0.1Ga0.9N/GaN triple quantum well laser," *Energy Procedia*, vol. 157, no. 75, 2019.

[30] L. Ömer, "Revealing the effects of nitrogen on threshold current density in GaNxAsyP1-x-y/GaP/AlzGa1-zP type I QW laser structures by hydrostatic pressure," *Physica E: Low-Dimensional Systems and Nanostructures*, vol. 81, p. 760, 2016.

[31] H. Zhao, G. Liu, J. Zhang, R. A. Arif, and N. Tansu, "Current injection efficiency induced efficiency droop in InGaN quantum well light emitting diodes," *Solid State Electron*, vol. 54, Article ID 1119, 2010.

[32] G. Liu, S. L. Chuang, and S. Park, "Optical gain of strained GaAsSb/GaAs quantum-well lasers: a self-consistent approach," *Journal of Applied Physics*, vol. 88, Article ID 5554, 2000.

[33] S. H. Park, "Optical gain of 1.3 mm GaAsSbN/GaAs quantum well lasers," *IET Optoelectronics*, vol. 1, no. 42, 2007.

[34] S. H. Park, "Optical gain characteristics in 1.55-μm GaAsSbN/GaAs quantum well structures," *Journal of the Korean Physical Society*, vol. 50, p. 1152, 2007.

[35] B. Chen and A. L. Holmes Jr., "Optical gain modeling of InP based InGaAs(N)/GaAsSb type-II quantum wells laser for mid-infrared emission," *Optical Quantum Electronics*, vol. 45, p. 127, 2013.

[36] B. Chen, "Optical gain analysis of GaAs-based InGaAs/GaAsSbBi type-II quantum wells lasers," *Optics Express*, vol. 25, Article ID 25183, 2017.

[37] J. Jiang and J. Sun, "Calculation of enhanced direct-gap optical gain in uniaxial tensile strained and n+-doped Ge/GeSi quantum well," *Advanced Photonics*, vol. paper JTu4A.1, 2016.

[38] W. Huang, H. Yang, B. Cheng, and C. Xue, "Theoretical study of the effect of different n-doping elements on band structure and optical gain of GeSn alloys," *Physical Chemistry Chemical Physics*, vol. 19, no. 39, pp. 27031–27037, 2017.

[39] I. H. Guizani and A. A. Rebey, "Spontaneous emission rate and radiative current density in p-GaAs/i-GaNAsBi/n-GaAs quantum well lasers," *Journal of Computational and Theoretical Nanoscience*, vol. 16, no. 11, pp. 4474–4478, 2019.

[40] S. L. M. van Mensfoort, J. Billen, M. Carvelli, S. I. E. Vulto, R. A. J. Janssen, and R. Coehoorn, "Predictive modeling of the current density and radiative recombination in blue polymer-based light-emitting diodes," *Journal of Applied Physics*, vol. 109, no. 6, Article ID 064502, 2011.

[41] C. Bilel and A. Rebey, "Optical absorption of new n-doped GaN0.38yAs1- 1.38ySby/GaAs QWs suitable for the design of 0.8 -1 eV solar cells," *International Journal of Control, Energy and Electrical Engineering (CEEE)*, vol. 9, p. 20, 2019.